Chinese Journal of Electronics
vol. 33, no. 2, pp. 472–478, March 2024
https://doi.org/10.23919/cje.2022.00.298

RESEARCH ARTICLE

A Novel Approach of Electromagnetic Compatibility Conducted Susceptibility Analysis Based on Gaussian Even Pulse Signal

Youwei MENG[1,3], Yanhua PENG[1,3], Haoyang ZHANG[1,3], Lilin LI[2,3], and Donglin SU[1,2,3]

1. *The School of Electronic and Information Engineering, Beihang University, Beijing 100191, China*
2. *The Research Institute for Frontier Science, Beihang University, Beijing 100191, China*
3. *The Institute of Electromagnetic Compatibility Technology, Beihang University, Beijing 100191, China*

Corresponding author: Lilin LI, Email: lll_work@buaa.edu.cn
Manuscript Received September 1, 2022; Accepted January 6, 2023

Abstract — The purpose of the electromagnetic compatibility conducted susceptibility test for interconnected cables in the system is to evaluate its ability to operate acceptably when subjected to interference. We propose a novel conducted susceptibility analysis approach: by injecting the Gaussian even pulse signal, we find that the susceptibility threshold of the system shows two different patterns with the change of signal parameters; then we locate the cause of the susceptibility of the device by analyzing the threshold level curves. The effectiveness of the proposed approach is verified by testing with devices containing digital modules such as navigation receivers. The proposed approach facilitates a deeper understanding of the susceptibility mechanism of systems and their appropriate electromagnetic compatibility design.
Keywords — Electromagnetic compatibility, Conducted susceptibility, Gaussian even pulse, Threshold level curves.
Citation — Youwei MENG, Yanhua PENG, Haoyang ZHANG, *et al.*, "A Novel Approach of Electromagnetic Compatibility Conducted Susceptibility Analysis Based on Gaussian Even Pulse Signal," *Chinese Journal of Electronics*, vol. 33, no. 2, pp. 472–478, 2024. doi: 10.23919/cje.2022.00.298.

I. Introduction

There are a large number of interconnected cables in the system, which are widely distributed, and the energy coupling to the cables could trigger electromagnetic susceptibility problems when operating [1], [2]. Awareness of the problems at the physical level is essential to improving their electromagnetic compatibility (EMC) capability, through conducted susceptibility (CS) test of interconnected cables in systems or devices [3].

The generally accepted test method is the CS test regulated in MIL-STD-461, which injects a certain energy signal into the cable of the equipment under test (EUT) through a current probe to test the ability of the EUT to withstand interference signals [4]–[6]. Frequency-domain test methods use signals such as sine waves and damped signals, which analyze conducted susceptibility from the perspective of discrete frequency power differences. These methods cannot simulate the real operating environment of the EUT, so there is a limitation in the perception of device susceptibility in broadband interference environment [7], [8]. Reference [9] proposed the multi-frequency CS test method, which injects multiple frequency points simultaneously and can greatly improve test efficiency.

Existing research on EMC time-domain detection mainly focuses on methods and test instruments [10], [11]. The concept of time-domain electromagnetic interference (EMI) detection was first proposed by Bronaugh [12], who believed that it was an effective solution to maximize the simulation of the real operating environment of the device and reflect its real susceptibility characteristics. References [13]–[15] focused on obtaining time-domain interference from the environment, and they analyzed signals such as surges, electrical fast transients, and electrostatic discharges. Then they found that the broadband time-domain pulses were the dominant interference waveform. The time-domain EMI measurement

Associate Editor: Prof. Yinghong WEN, Beijing Jiaotong University.

receiver developed by Russer gives more EMI information [16], [17]. In addition, his team developed a real-time broadband time-domain EMI measurement system with a frequency band covering 30 MHz to 1000 MHz, which shortened the test time compared to the conventional methods [18]–[20]. Reference [21] developed a time-domain measurement system to handle the limitations of the amplitude probability detector. Reference [22] used digital signal processing techniques to improve the EMI assessment of time-domain measurement instruments. The above research shows that time-domain signals play an important role in CS tests. However, the scarcity of methods and systems has prevented this signal from being used on a large scale.

In this paper, we deepen the idea of simultaneous injection of multiple frequency points into using time-domain pulse signals. Based on the powerful stimulating susceptibility ability of the hardware system developed in [23], we stimulate the sensitive phenomena not found in the CS114 test, and then define the susceptibility profile by plotting threshold level curves (TLC). We found that the TLC of EUT showed two different patterns with the variation of signal parameters, which can provide sufficient data to support the explanation of the susceptibility mechanism.

The remainder of this paper is organized as follows: Section II introduces the proposed analysis approach and the two interference patterns found for the devices containing digital modules; Section III presents the test with the navigation receiver as EUT; Section IV analyzes the test results and provides a detailed description of the patterns and Section V gives the conclusion.

II. The Time-Domain Test Approach and Susceptibility Pattern Cognition

1. Time-domain signal selection

The real operating electromagnetic environment of the device may have multiple signals and contain multiple frequencies at the same time. Gaussian even pulse signal has the characteristics of rich frequency content and wide spectral distribution, which can be used to effectively simulate the real environment, more likely to inspire the electromagnetic susceptibility of the EUT. The Gaussian even pulse is composed of two Gaussian pulses with equal amplitude, opposite polarity, and pulse spacing of δ. The time-domain expression is

$$w(t)=A\exp\left[-\frac{1}{2}\left(\frac{t-T_c}{\alpha}\right)^2\right]-A\exp\left[-\frac{1}{2}\left(\frac{t-T_c-\delta}{\alpha}\right)^2\right] \tag{1}$$

The Fourier transform of (1) is given by

$$|F(f)|=\frac{2A}{\sqrt{2\pi}f_c}\left|\sin\left(\frac{f\delta}{2f_c}\right)\right|\exp\left[-\frac{1}{2}\left(\frac{f}{f_c}\right)^2\right] \tag{2}$$

The frequency spectrum of the Gaussian even pulse has several depression points and the distribution range changes with the pulse spacing. Taking advantage of this property, the frequency-domain susceptibility range of the EUT is determined while injecting the Gaussian even pulse signal with different pulse spacing in the time domain. Therefore, the first adjustable parameter of the Gaussian even pulse signal is the pulse spacing δ. Secondly, the pulse repetition frequency F_r indicates the number of pulses injected per unit of time, which can be used to calculate the time associated with the operation of the device. Finally, the susceptibility profile of the EUT is directly related to the amplitude of the signal, so the amplitude A_m of the Gaussian signal should also be concerned. The proposed approach facilitates a deeper understanding of the susceptibility mechanism of EUT through the patterns that the TLC of presents.

We simulate and measure the waveform of the Gaussian even pulse, and the results are compared in Figure 1. It can be seen that the ideal Gaussian even pulse is without the consideration of the trailing and can precisely modulate the amplitude A_m.

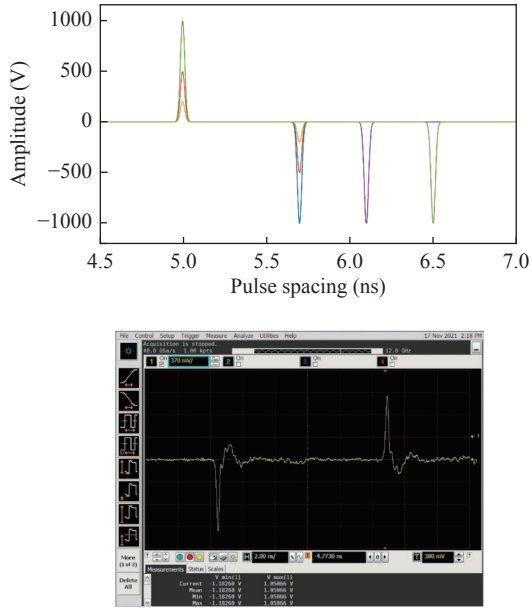

Figure 1 The comparison of Gaussian even pulse simulation results (above) and measurement results (below). Different color curves correspond to the Gaussian even pulse with different spacing and amplitude parameters.

The susceptibility threshold is the critical signal amplitude that makes the device sensitive, the susceptibility threshold level should be determined when the sensitive phenomenon just does not appear. In this paper, it is the constant Gaussian signal spacing δ and repetition frequency F_r, corresponding to the minimum signal amplitude A_m that can stimulate susceptibility. Adjusting the pulse spacing, we can obtain the curves for the variation of the threshold with δ. The TLC can reflect the susceptibility profile of the device. Here we analyze the two

patterns of the TLC.

2. Susceptibility pattern study

We have analyzed the results of numerous experiments on various EUT with digital modules and found that their TLC of susceptibility shows two patterns under the effect of Gaussian even pulse: one is that the curves show a cluster effect with the gradual increase of the repetition frequency, as shown in Figure 2; the other one is that the susceptibility threshold decreases with increasing repetition frequency, as shown in Figure 3.

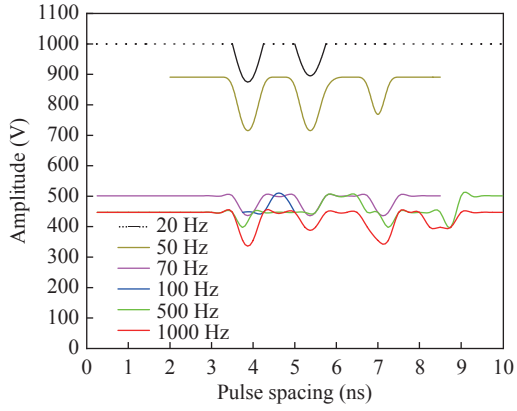

Figure 2 Time-domain threshold level curves of susceptibility for IPL. When the repetition frequency F_r exceeds 70Hz, the curves appear as a cluster. The susceptibility threshold is no longer strongly correlated with the F_r.

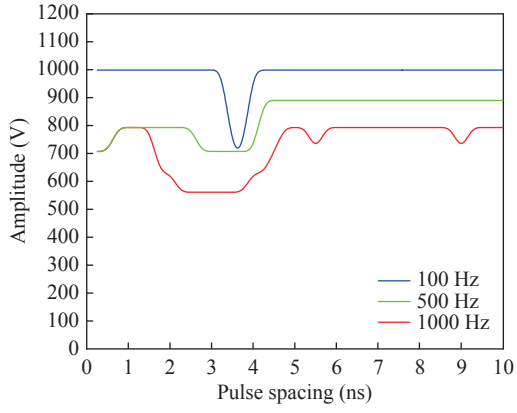

Figure 3 Time-domain threshold level curves of susceptibility for ISL. The susceptibility threshold is negatively correlated with the F_r.

These patterns present two different types of interference. The first pattern reflects the interference on the physical layer (IPL), where the Gaussian pulse signal acts on the circuit of EUT, causing transient failure and restarting through a higher transient peak.

Due to the large transient voltage of the Gaussian pulse, the injection causes transient fault or protection in the signal processing circuit, which takes some time to recover. When the repetition period of the pulse signal (the time corresponding to the repetition frequency F_r) is greater than the time required for the system to recover, the large peak voltage is required for the receiver to stimulate susceptibility, and this value decreases as the F_r increases. When the repetition period is less than or equal to the circuit recovery time, the susceptibility threshold of the EUT is no longer strongly correlated with the F_r, because the processing circuit cannot recover in time at different signal repetition frequencies and the threshold level curves exhibit clustering. The dashed part of the black line in Figure 2 indicates that the EUT still operating normally when the amplitude of the pulse is adjusted to the maximum.

The second pattern reflects the interference on the signal layer (ISL), where the Gaussian pulse signal acts on information transmitted by the cable, resulting in a high bit error rate at the receiver and making it difficult to decode.

There is no cluster of curves for ISL. In a certain range, the susceptibility threshold of the EUT is negatively correlated with the repetition frequency of the pulse. The regularity can be intuitively understood that the Gaussian pulse directly affects the signal transmitted on the cable. The greater the F_r, the more severely the signal is interfered with, which allows the excitation of sensitive phenomena with a smaller voltage threshold.

III. Examples of Application

To verify the two interference patterns mentioned in Section II, we carried out experiments with a navigation receiver system as the EUT using the connection schematic in Figure 4. The pulse source is used to generate Gaussian even pulse with an adjustable repetition frequency F_r and pulse spacing δ. The amplitude A_m of the pulse is controlled by the adjustable attenuator, and the signal is subsequently injected into the test cable of the EUT through the left probe. To maintain a basic test setup for the EUT and minimize errors, we locate the monitoring probe 5 cm from the connector and positioned the injection probe 5 cm from the monitor probe. The three-parameter ranges are [1 Hz, 1000 Hz], [0 ns, 10 ns], [0 V, 1000 V]. The monitoring probe near the EUT is connected to an oscilloscope, which is used to observe whether the pulse signal is effectively injected.

The attenuator, oscilloscope, and probe used in Figure 4 are 50 Ω impedance matching, and they are connected using the coaxial transmission line with 50 Ω characteristic impedance. Before starting the test, the normal function of the EUT should be tested.

The test procedures shall be as follows:

1) Connect the EUT with measurement devices according to Figure 4 and select the test cable.

2) Initialize the parameters of the Gaussian even pulse signal generator. Test with lower parameter values and then gradually increase the F_r and A_m until observing the susceptibility.

3) Reduce the signal amplitude A_m until the EUT returns to normal, and then continue to reduce the signal amplitude by 6 dB, and gradually increase the level until the sensitive phenomenon just repeats, and record

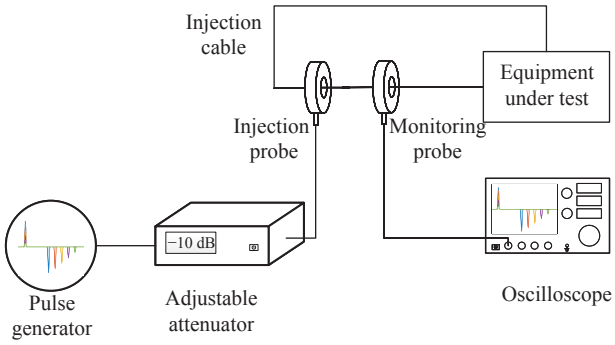

Figure 4 The test schematic.

the signal parameters. Change the parameters and repeat the above operation.

4) Construct the profile of susceptibility by plotting time-domain and frequency-domain threshold level curves based on the accumulated data.

5) Analyze the susceptibility mechanism of the EUT according to the pattern of curve presentation.

The navigation receiver system is mainly composed of the receiver, transponder monitor, and antennas of the satellite signal. Due to the low power of the satellite signal received on the ground and its susceptibility to interference, the test was conducted in a microwave darkroom, to ensure the accuracy of the result. The test scenario is shown in Figure 5.

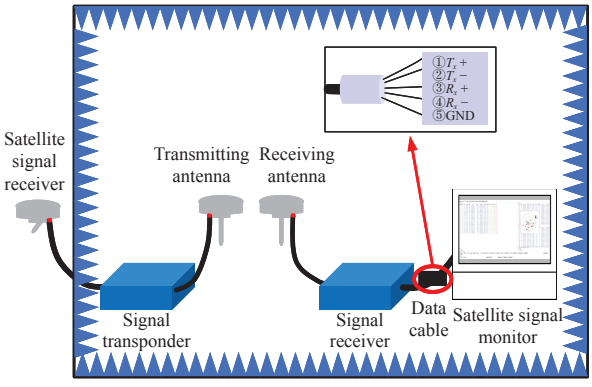

Figure 5 The cable diagram of the navigation receiver.

The reference standard is the number of participating satellites shown on the monitor. The number of satellites involved in positioning is five or more during normal operation, and if the number is less than these will lead to positioning failure, for which we record the symbol "Y". On the contrary, there is no susceptibility, defined as "N". The test results recorded for typical parameters are shown in Table 1. A_t is the value of the attenuator, and the A_m is the maximum amplitude minus it.

The test system has a corresponding control algorithm that modulates the spacing and amplitude of the next pulse based on the presence or absence of susceptibility after each injection. Combined with the maximum spacing that the system can achieve, and the minimum step, a maximum number of tests is given.

Table 1 The CS test of data cable for receiver

No.	A_t (dB)	F_r (Hz)	δ (ns)	Stimulate susceptibility
1	2	20	4	N
2	2	70	4	Y
3	7	70	4	N
4	7	500	4	Y
5	7	500	6	N
6	8	1000	4	Y
7	8	1000	6	N
8	8	1000	7.25	Y

IV. Results Analysis

Based on the results obtained in Section III, the time-domain and frequency-domain susceptibility threshold curves can be plotted. Taking the blue curve in Figure 2 as an example, when the injected Gaussian pulse signal with a repetition frequency of 1000 Hz, if the signal point is above the blue curve, there will be a problem with the device of susceptibility, like the eighth result in Table 1. Converting the parameters of the points from the time-domain to the frequency-domain gives the cluster of curves in different colors in Figure 6. The red curve obtained by taking the upper envelope of this cluster of curves is the frequency-domain threshold level curves of susceptibility. If the broadband signal power in the environment lies above the frequency-domain TLC, there will be a problem with the device of susceptibility as well.

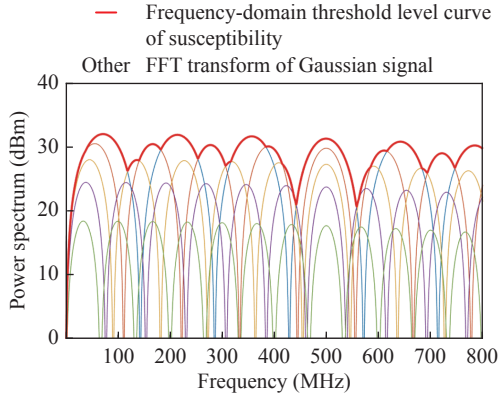

Figure 6 The signal power spectrum of susceptibility for the navigation receiver system. Converting the parameters of the test points from the time-domain to the frequency-domain gives the cluster of curves in different colors. The red curve is obtained by taking the upper envelope of this cluster of curves, which is the frequency-domain threshold level curves of susceptibility.

1. Interference on physical level

It should be noted that the points below the red curve in Figure 6 do not mean that no susceptibility will be induced, because the red curve is obtained by taking the upper envelope, and some of these clustered frequency-domain signal curves are located completely below the

envelope. In the following, we analyze and verify two interference patterns.

For the susceptibility of the navigation receiver in Section III, it can be inferred that the interference generated is the physical layer. For the IPL, the threshold level of susceptibility is almost similar when the repetition frequency of the Gaussian pulse signal is high.

To further find out the dividing frequency of the threshold curve into clusters, we used three kinds of pulse spacing of 4.0 ns, 5.5 ns, and 7.0 ns as examples to test and the result is shown in Figure 7, which repetition frequency of 70 Hz is a clear inflection point, corresponding to the repetition time of 14.3 ms.

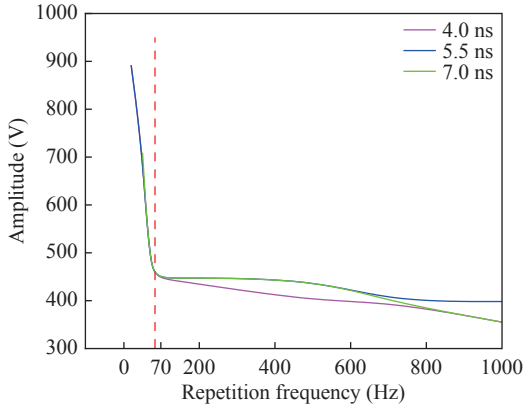

Figure 7 The variation of the threshold level of susceptibility with the repetition frequency for the navigation receiver. The red dotted line represents that the repetition frequency is 70 Hz, which is the obvious inflection point common to all three curves.

Analysis of the navigation receiver interfered causes are as follows: the injection position of the test pulse is the signal cable at the rear of the satellite signal receiver, which uses the USB 2.0 protocol to transmit information to the monitor. Before the monitor communicates with the receiver, it sends a reset signal for initialization, which sets the level on both positive and negative signal cables to zero, and the state is maintained for 10 ms by default. Therefore, the reconnection time between them after the interference is slightly more than 10 ms, which is very close to the experimental 14.3 ms and verifies the correctness of the conclusion obtained.

2. Interference on signal level

We use an electric vehicle as the EUT for the verification of ISL. The vehicle makes corresponding actions according to the commands issued by the remote control. Figure 8 shows a picture of the electric vehicle testing.

It was found that as the repetition frequency of the Gaussian pulse increases, the electric vehicle may exhibit different susceptibilities. If the four different phenomena are quantified to four levels according to severity, the most serious susceptibility disconnected from the control system is recorded as the number 4, accordingly, delayed control signal is recorded as 3, failure to follow instructions to complete actions is recorded as 2, and operating normally is recorded as 1. The variation of the susceptibility level of the electric vehicle with the repetition frequency is shown in Figure 9.

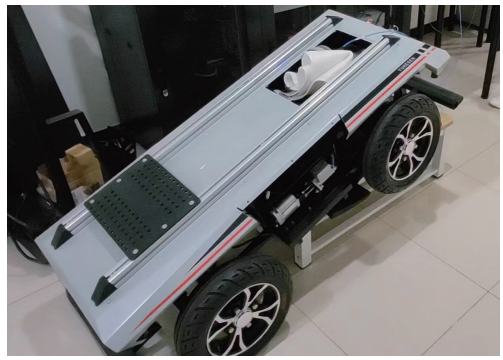

Figure 8 The picture of tested electric vehicle.

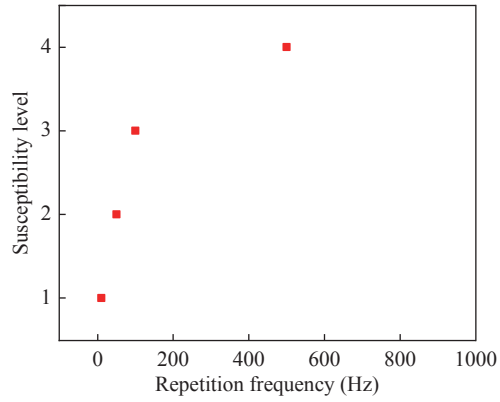

Figure 9 The variation of the susceptibility level with the repetition frequency for the electric vehicle. The level of susceptibility escalates with repetition frequency increasing, which means the situation gets progressively worse.

As can be seen from Figure 9, the level of susceptibility exhibited by the electric vehicle increases as the repetition frequency of the injected Gaussian pulse increases, which means the situation gets progressively worse. In this process, the size of the repetition frequency value is like the level of environmental noise, which has an interference effect on the command signal sent by the remote control. When the value is low, although the instruction has interfered, but still can be transmitted to the receiver, but the interfered instruction is not the same as when it was sent, so there is level 2 of susceptibility. As the value increases, the command signal is gradually drowned, and the receiver cannot receive the control command, so level 4 of susceptibility appears. It is further verified that the interfering signal impacts the signal layer by affecting the bit error rate of the transmitted command for the electric vehicle.

Since the proposed method is mainly oriented to conducted susceptibility testing of cables, we have compared it with the traditional frequency-domain test method CS114, as shown in Table 2. For example, in the CS114, assuming an injection time of 10 s for each point, 2183 frequency points are required for testing in the

band of 10 kHz–400 MHz, with a maximum frequency interval of 1 MHz. However, our tests according to the standard did not stimulate the susceptibility of the navigation receiver. The proposed method not only has the ability to stimulate susceptibility of the EUT, but also the number of points and time used for the test has obvious advantages, which greatly improves the efficiency of CS test.

Table 2 The comparison of the proposed approach and the CS114 approach

Test approach	Cables	Stimulate susceptibility	Time (s)
Proposed aproach	Tx	*Y*	210
	Rx	*Y*	210
	GND	*N*	1400
CS114 approach	Tx	*N*	21830
	Rx	*N*	21830
	GND	*N*	21830

V. Conclusion

In this paper, we propose an approach to analyze the susceptibility mechanism of EMC conduction based on the time-domain Gaussian pulse signal. The Gaussian even pulse is used as the test signal to stimulate sensitive phenomena, then the large amount of data obtained from the test helps to determine the cause of the susceptibility of the EUT. For the two interference patterns, the interference on the physical layer and signal layer, we summarize and verify their regularity, which helps to improve our knowledge of the susceptibility mechanism of the digital modules or systems. The approach proposed in this paper can provide support for modeling, simulation, and theoretical research on CS. It also proposes a new inspiration for CS test and analysis, which has important theoretical and application value.

Acknowledgement

This work was supported in part by the National Natural Science Foundation of China (NSFC) (61427803, 62201021).

References

[1] D. L. Su, S. G. Xie, F. Dai, *et al.*, *Theory and Methods of Quantification Design on System-Level Electromagnetic Compatibility*, Springer, Singapore, pp.55–56, 2019.

[2] G. Lugrin, S. V. Tkachenko, F. Rachidi, *et al.*, "High-frequency electromagnetic coupling to multiconductor transmission lines of finite length," *IEEE Transactions on Electromagnetic Compatibility*, vol. 57, no. 6, pp. 1714–1723, 2015.

[3] L. Freeman and T. Wu, "Method for derivation and synthesis of conducted susceptibility limits for system-level EMC," *IEEE Transactions on Electromagnetic Compatibility*, vol. 58, no. 1, pp. 4–10, 2016.

[4] GJB 151B-2013: 2013, Equipment Development Department of People's Republic of China Central Military Commission, Electromagnetic emission and susceptibility requirements and measurements for military equipment and subsystems.

[5] MIL-STD-461G: 2015, U.S. Department of Defense, Requirements for the control of electromagnetic interference characteristics of subsystems and equipment.

[6] H. Teimourzadeh, B. Mohammadi-Ivatloo, and M. Shahidehpour, "Adaptive protection of partially coupled transmission lines," *IEEE Transactions on Power Delivery*, vol. 36, no. 1, pp. 429–440, 2021.

[7] W. Wang, F. Zhang, Z. H. Zhao, *et al.*, "A novel method for extracting broadband component of electromagnetic emission," in *Proceedings of the 2020 IEEE MTT-S International Wireless Symposium*, Shanghai, China, pp.1–3, 2020.

[8] L. Fu, Z. W. Yan, C. S. Fu, *et al.*, "Extraction and analysis of conducted electromagnetic susceptibility elements of integrated circuits," *IEEE Access*, vol. 9, pp. 149125–149136, 2021.

[9] T. Huang, D. L. Su, and H. T. Sun, "Uncertainty analysis in conduction susceptibility of cable injection test," in *Proceedings of the 2011 International Conference on Electrical and Control Engineering*, Yichang, China, pp.5145–5147, 2011.

[10] S. L. Tantum and L. M. Collins, "A comparison of algorithms for subsurface target detection and identification using time-domain electromagnetic induction data," *IEEE Transactions on Geoscience and Remote Sensing*, vol. 39, no. 6, pp. 1299–1306, 2001.

[11] F. Krug and P. Russer, "Ultra-fast broadband EMI measurement in time-domain using FFT and periodogram," in *Proceedings of the 2002 IEEE International Symposium on Electromagnetic Compatibility*, Minneapolis, MN, USA, pp.577–582, 2002.

[12] E. L. Bronaugh and J. D. M. Osburn, "New ideas in EMC instrumentation and measurement," in *Proceedings of the 10th International Zurich Symposium On Electromagnetic Compatibility*, Zurich, Switzerland, pp.323–326, 1993.

[13] G. Spadacini, T. Liang, F. Grassi, *et al.*, "Worst case and statistics of waveforms involved in wideband intentional electromagnetic attacks," *IEEE Transactions on Electromagnetic Compatibility*, vol. 60, no. 5, pp. 1436–1444, 2018.

[14] C. F. M. Carobbi, A. Bonci, M. Stellini, *et al.*, "Time-domain characterization of the surge, EFT/Burst, and ESD measurement systems," *IEEE Transactions on Instrumentation and Measurement*, vol. 62, no. 6, pp. 1840–1846, 2013.

[15] S. W. Lim, S. Katsuki, Y. S. Jin, *et al.*, "Nanosecond high-voltage pulse generator using a spiral blumlein PFL for electromagnetic interference test," *IEEE Transactions on Plasma Science*, vol. 42, no. 10, pp. 2909–2912, 2014.

[16] S. Braun, M. Al-Qedra, and P. Russer, "A novel realtime time-domain EMI measurement system based on field programmable gate arrays," in *Proceedings of the 17th International Zurich Symposium on Electromagnetic Compatibility*, Singapore, pp.501–504, 2006.

[17] C. Hoffmann and P. Russer, "A real-time low-noise ultrabroadband time-domain EMI measurement system up to 18 GHz," *IEEE Transactions on Electromagnetic Compatibility*, vol. 53, no. 4, pp. 882–890, 2011.

[18] P. Russer, "EMC measurements in the time-domain," in *Proceedings of the 2011 XXXth URSI General Assembly and Scientific Symposium*, Istanbul, Turkey, pp.1–35, 2011.

[19] F. Krug and P. Russer, "The time-domain electromagnetic interference measurement system," *IEEE Transactions on Electromagnetic Compatibility*, vol. 45, no. 2, pp. 330–338,

2003.

[20] S. Braun, T. Donauer, and P. Russer, "A real-time time-domain EMI measurement system for full-compliance measurements according to CISPR 16-1-1," *IEEE Transactions on Electromagnetic Compatibility*, vol. 50, no. 2, pp. 259–267, 2008.

[21] M. Pous and F. Silva, "Full-spectrum APD measurement of transient interferences in time domain," *IEEE Transactions on Electromagnetic Compatibility*, vol. 56, no. 6, pp. 1352–1360, 2014.

[22] M. A. Azpúrua, M. Pous, S. Çakir, *et al.*, "Improving time-domain EMI measurements through digital signal processing," *IEEE Electromagnetic Compatibility Magazine*, vol. 4, no. 2, pp. 82–91, 2015.

[23] D. L. Su, Y. H. Peng, L. L. Li, *et al.*, "A broadband time-domain detection system for electromagnetic compatibility conducted susceptibility test," *IEEE Transactions on Instrumentation and Measurement*, vol. 71, article no. 3000811, 2022.

Youwei MENG received the B.S. degree in electronic and information engineering in 2019 from the Beihang University, Beijing, China, where he is currently working toward the Ph.D. degree in information and communication engineering. His research interests include electromagnetic compatibility, electromagnetic interference, adjacent channel interference and active filters.
(Email: mengyouwei@buaa.edu.cn)

Yanhua PENG received the B.E. degree in communication engineering from Harbin Engineering University, Harbin, China in 2017, received the M.E. degree in communication and information system from University of Chinese Academy of Sciences, Beijing, China in 2020. He is currently working toward the Ph.D. degree at the Institute of EMC, Beihang University, Beijing, China. His research interests include electromagnetic compatibility and electromagnetic environment.

Haoyang ZHANG received the B.E. degree in electronic and information engineering in 2020 from Beihang University, where he is currently pursuing the Ph.D. degree in circuits and systems. He joined the Institute of Electromagnetic Compatibility Technology in 2020. His current research interests include electromagnetic compatibility, electromagnetic optimization design and evolutionary computation.

Lilin LI received the B.S. and Ph.D. degrees from Beihang University in 2017 and 2021, respectively. She joined the Research Institute for Frontier Science, Beihang University in 2021, and is working as a Research Associate currently. Her research interests include electromagnetic compatibility design in system level and optimizations in the electromagnetic.
(Email: lll_work@buaa.edu.cn)

Donglin SU received the B.S., M.S., and Ph.D. degrees in electrical engineering from Beihang University (BUAA), Beijing, China, in 1983, 1986, and 1999, respectively. In 1986, she joined the Faculty of School of Electronics and Information Engineering, BUAA, where she was first an Assistant, then a Lecturer, later on an Associate Professor, and is currently a Full Professor. From 1996 to 1998, she was a Visiting Scholar with the Department of Electrical Engineering, University of California, Los Angeles, CA, USA, under the BUAA-UCLA Joint Ph.D. Program. She has authored more than 100 papers and coauthored several books. Her research interests include the numerical methods for microwave and millimeter-wave integrated circuits and systematic electromagnetic compatibility design of various aircrafts. Dr. Su is a Member of the Chinese Academy of Engineering. She is a Fellow of the Chinese Institute of Electronics (CIE). She is the Chair of Beijing Chapter of the IEEE Antennas and Propagation Society and the Deputy Chair of the Antennas Society, CIE. She was the recipient of the National Science and Technology Advancement Award of China in 2007 and 2012, and the National Technology Invention Award of China in 2018.